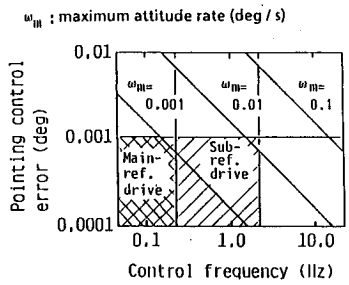

Fig. 2 Control regions of two reflector drive methods.

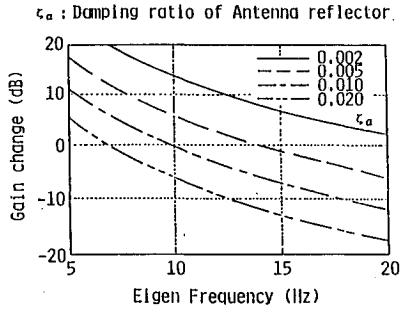

Fig. 3 Relations between control gain change and structural parameters.

Antenna Structure Dynamics

Large onboard antennas, which are stowed during launch, are deployed once the satellite reaches its designated orbit. Reflectors are supported with antenna support booms and deployment mechanisms. For satellite communications using the Ka or Ku band, the subreflector itself is rigid in comparison with the drive control frequency. However, the antenna support booms with deployment mechanisms are flexible. The antenna structures, therefore, can be modeled as a flexible cantilever with a rigid mass and a torque actuator at its tip. To prevent these structures from resonating, their eigenfrequencies must be greater than the control frequency of the ADCS. On the other hand, very high eigenfrequencies require the structure mass to be increased. To optimize the system, it is important to identify clearly the dynamics of these structures. In this study, the influences of structural parameters on control gain of the ADCS are assessed for the gain stabilization control concept.

Satellite dynamics can be ignored in the antenna pointing control system of ETS-VI because the attitude control frequency is lower than one-tenth of the antenna drive control frequency and the inertia of the satellite main body is much larger than that of the driven subreflector. The dynamics of the antenna structures, therefore, are given by

$$I_a\ddot{\theta}_a + I_a\phi_a'\ddot{q} = T_{ac} \tag{2}$$

$$I_a\phi_a'\ddot{\theta}a + m\ddot{q} + 2\zeta_a\omega_n\dot{q} + \omega_n^2 q = 0 \tag{3}$$

$$\theta_p = K_b(\theta_a + \phi_a' q + r\phi_a q) \tag{4}$$

where $m = 1 + I_a\phi_a'^2 + m_a\phi_a^2$, in which m_a is a mass that is driven. The transfer function of these structures, $G_p(s)$, is derived using Eqs. (2-4).

$$G_p(s) = \frac{K_b}{I_a s^2}\,\frac{bs^2 + 2\zeta_a\omega_n s + \omega_n^2}{as^2 + 2\zeta_a\omega_n s + \omega_n^2} \tag{5}$$

where

$$a = \frac{1 + m_a\phi_a^2}{m} \tag{6a}$$

$$b = \frac{1 + m_a\phi_a^2 - I_a\phi_a' r\phi_a}{m} \tag{6b}$$

In Eq. (5), the term in parentheses represents the flexibility of the antenna structures. The gain at the eigenfrequency of the structures, $\omega_n/a^{1/2}$, is given by

$$G = \frac{K_b a}{I_a\omega_n^2}\,\frac{[a(1 - b/a)^{1/2} + 4\zeta_a^2]}{4\zeta_a^2} \tag{7}$$

To maintain sufficient gain margin in the ADCS at the resonant frequency, gain changes due to deviations in structural parameters are calculated. Figure 3 shows gain changes vs eigenfrequencies for four damping ratios. In our assessment, the nominal value of Z_a is 0.01, and its tolerance is about 0.005. The gain change is, therefore, calculated to be about 6 dB. Other flexible parameters, modal slope and modal displacement angle, were estimated in a similar manner. The control gain changes due to these tolerances were clarified as about 3 and 2 dB, respectively. As a result, a gain margin of more than 11 dB is required to make the control system stable against changes in the structural parameters.

Conclusion

Significant structural parameters of the onboard antenna pointing control system for ETS-VI were clarified, and the following conclusions were reached.

1) A subreflector drive is preferable to a main-reflector drive, because of required control accuracy and total antenna mass.

2) A control gain margin of about 11 dB is necessary for the control system to be stabilized against changes in the structural parameters.

Calculation of Stability Derivatives for Slender Bodies Using Boundary Element Method

Shinji Suzuki* and Kizuki Fukuda†
University of Tokyo, Tokyo, Japan

Introduction

THIS Note presents the application of the boundary element method to calculate the stability derivatives for a slender body. Aerodynamic characteristics of slender fuselages, wings, and their combinations have been estimated using the slender-body theory in the initial design stage.[1] This theory can transform three-dimensional flow problems into two-dimensional, incompressible flow problems in the crossflow plane perpendicular to the long axis of the body.[2,3] Bryson has shown that the theoretical stability derivatives of the slender body could be determined by use of the concept of apparent-mass coefficients of the crossflow section of the slender body.[4] However, since the conformal mapping technique has been used to analyze the two-dimensional flow, it has been difficult to calculate the stability derivatives of a complicated configuration by the slender-body theory. In the present Note, the boundary element method[5] is applied to

Received Oct. 4, 1988; revision received May 29, 1989.

*Associate Professor, Department of Aeronautics.
†Graduate Student, Department of Aeronautics.

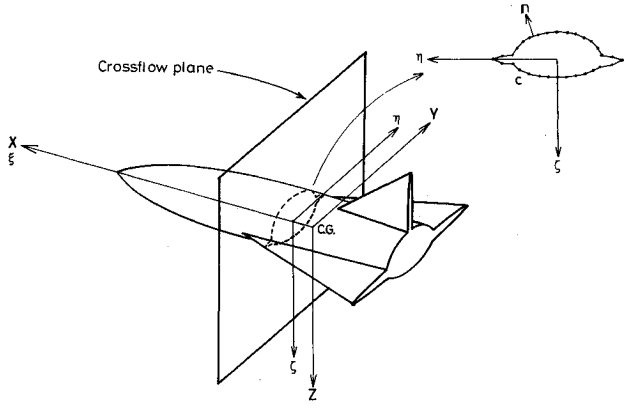

Fig. 1 Coordinate system and element division of crossflow section.

calculate the apparent-mass coefficients of the crossflow section with an arbitrary shape to estimate the stability derivatives.

Slender-Body Theory

Figure 1 shows a typical slender body moving in an infinite fluid, stationary at infinity. Let the body axes X, Y, and Z have their origins fixed at the center of the gravity of the body. The local axes ξ, η, and ζ are defined on the crossflow plane as shown in Fig. 1. Here, configurations are limited to ones where the aft end of the fuselage and all wing trailing edges lie in the bottom crossflow section.

In this Note, the flow about the body is analyzed using the slender-body theory. The basic thought underlying this theory is the assumption that changes in the perturbation velocities about the bodies are small in the X direction compared with those of the perturbation velocities in the Y and Z directions. This causes the potential equation to be reduced to that of two-dimensional flows in the η-ζ plane (the crossflow plane). Therefore, the disturbance potential in the crossflow plane can be given by

$$\phi = v\phi_1 + w\phi_2 + p\phi_3 + \sum_{i=1}^{r} u_i\phi_{3+i} \tag{1}$$

where v and w are the velocities of the crossflow section in the η and ζ directions, and p is the angular velocity of the crossflow section about the ξ axis. Furthermore, u_i is the velocity of the ith control surface in the crossflow section.

The kinetic energy of the fluid per unit length along the X axis is given by

$$T = \tfrac{1}{2}\, q^t M q \tag{2}$$

where

$$q^t = [v, w, p, u_1, u_2, \ldots, u_r] \tag{3}$$

$$M_{ij} = -\rho \int_c \phi_i \frac{\partial \phi_j}{\partial n}\, ds \qquad (i,j = 1,2,3,\ldots,3+r) \tag{4}$$

and c, ρ, and n are the boundary surface of the body in the crossflow plane, the density of the fluid, and the outward unit normal vector defined on c as shown in Fig. 1, respectively. Note that M_{ij} are called the apparent-mass coefficients of the crossflow section.

Bryson's method of apparent masses is based on the results of Lamb,[6] which indicate that the aerodynamic force per unit length on the body at a crossflow section can be evaluated by using the kinetic energy in Eq. (2). The total aerodynamic forces and moments acting on the body are calculated by integrating the sectional forces from the base to the apex along the X axis.[4]

Boundary Element Calculation

The disturbance potential in a two-dimensional incompressible flow is governed by the following integral equation[5]:

$$\frac{1}{2}\phi + \frac{1}{2\pi}\int_c \phi \frac{\partial}{\partial n}\left(\ell n \frac{1}{r}\right) ds = \frac{1}{2\pi}\int_c \frac{\partial \phi}{\partial n}\ell n\left(\frac{1}{r}\right) ds \tag{5}$$

where r is the distance between any two points on the boundary surface.

So as to solve Eq. (5) numerically, the boundary is divided into N segments (Γ_i) as shown in Fig. 1. The values of ϕ_i, $\partial\phi_i/\partial n$ are then assumed to be constant on each element. If collocation points are selected at the middle of each element, Eq. (5) is finally rewritten as follows[5]:

$$HU = GQ \tag{6}$$

where

$$H_{ij}\begin{cases} = \dfrac{1}{2\pi}\displaystyle\int_{\Gamma_j} \frac{\partial}{\partial n}\ell n\left(\frac{1}{r}\right) ds & i \neq j \\ = \dfrac{1}{2} & i = j \end{cases} \tag{7a}$$

$$G_{ij} = \frac{1}{2\pi}\int_{\Gamma_j} \ell n\left(\frac{1}{r}\right) ds \tag{7b}$$

$$U = [\phi_1, \phi_2, \ldots, \phi_N] \tag{8}$$

$$Q = \left[\frac{\partial\phi_1}{\partial n}, \frac{\partial\phi_2}{\partial n}, \ldots, \frac{\partial\phi_N}{\partial n}\right] \tag{9}$$

It is noted that the Q is defined by the boundary conditions, which require that the normal component of the flow on the boundary surface should be zero. Hence, we can get U by

$$U = H^{-1}GQ \tag{10}$$

The apparent-mass coefficients in Eq. (4) can be calculated by integrating the product of vectors U and Q. The preceding numerical calculation makes it possible to obtain the apparent-mass coefficients of an arbitrarily shaped section.

Results and Conclusion

First, the apparent-mass coefficients of a circular body with a planar midwing were calculated. The planar wing was assumed to be an ellipse with a thickness ratio of 0.05. Boundary surfaces were divided into 48 segments. Two types of apparent-mass coefficients, M_{33} and M_{22}, are illustrated in Fig. 2, where the "circle" shows calculated results and solid lines indicate analytical solutions (Ref. 1, p. 372). The abscissa of Fig. 2 denotes the ratio of the radius of the body to the semispan of the wing. The ordinate means the apparent-mass coefficients, which are nondimensionalized by those of the wing without the body. This figure shows the high accuracy of the numerical method.

The second example was the stability derivatives of a flat triangular wing with analytical solutions. In the calculation, the cross section of the wing was assumed to be an ellipse with a thickness ratio of 0.05. The aspect ratio of the wing was selected to be 2.22. The center of moments, reference area, and reference length were adopted as the centroid of wing area, the wing planform, and the total wing span, respectively. Note that the angle of attack was chosen to be 0.1 rad. The cross section was divided into 48 segments and the number of cross sections along the X axis was 10. Table 1 compares calculated stability derivatives with analytically determined ones (Ref. 1, pp. 374–378.) This table indicates that the maximum error of the numerical results is less than 2%.

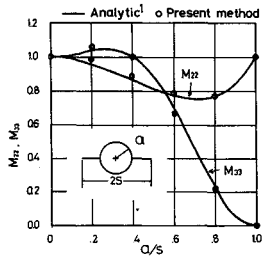

Fig. 2 Apparent-mass coefficient of planar midwing with body.

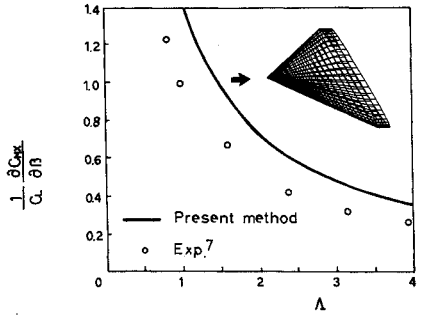

Fig. 3 Rolling moment due to sideslip of delta wings vs aspect ratio Λ.

Table 1 Stability derivatives of flat triangular wing[a]

	Analytic[1]	Present method
C_{yp}	0.209	0.211
$C_{z\alpha}$	−3.49	−3.51
C_{zq}	−2.09	−2.11
$C_{l\beta}$	−0.105	−0.104
C_{lp}	−0.218	−0.214
C_{lr}	−0.0157	−0.0156
C_{mq}	−0.471	−0.474
C_{np}	−0.0157	−0.0158

[a]Aspect ratio: 2.22; angle of attack: 0.1 rad.

Finally, the rolling moment due to the sideslip of the delta wings against the aspect ratio was computed to compare calculated results with experimental data.[7] As shown in Fig. 3, the profile of the cross section was an ellipse with a thickness ratio of 0.05 and was divided into 48 segments. In Fig. 3, the solid line denotes the calculated data and the "circle" means the experimental results (Ref. 7, p. 187). It is shown that the rolling moment due to the sideslip decreases greatly with the decreasing aspect ratio, and that agreement between measurements and calculation is good.

In summary, a simple computational method for the slender body theory has been developed to provide a computer-aided design tool for aerospace engineers who want to estimate the stability derivatives of an airplane with a slender body configuration at its initial design stage. It is finally noted that since the stability derivatives related to the drag force cannot be calculated by the preceding potential-flow theory, we use a semiempirical formula[1] for estimating the drag.[8]

References

[1]Nielsen, J. N., *Missile Aerodynamics*, McGraw-Hill, New York, 1960.

[2]Jones, R. T., "Properties of Low Aspect Ratio Pointed Wings at Speeds Below and Above the Speed of Sound," NACA Rept. 835, 1946.

[3]Spreiter, J. R., "The Aerodynamic Forces on Slender Plane and Cruciform-Wing and Body Combinations," NACA Rept. 962, 1950.

[4]Bryson, A. E., Jr., "Stability Derivatives for a Slender Missile with Application to a Wing-Body-Vertical-Tail Configuration," *Journal of the Aeronautical Sciences*, Vol. 20, No. 5, May 1953, pp. 297-308.

[5]Brebbia, C. A., and Walker, S., *Boundary Element Techniques in Engineering*, Newnes-Butterworth, London, 1980.

[6]Lamb, H., *Hydrodynamics*, 6th Ed., University Press, Cambridge, England, UK, 1963.

[7]Schlichting, H., and Truckenbrodt, E., *Aerodynamics of the Airplane*, translated by H. J. Ramm, McGraw-Hill, New York, 1979.

[8]Suzuki, S., and Fukuda, K., "Calculation of Stability Derivatives for Supersonic Airplanes and its Flight Dynamics (in Japanese)," *Proceedings of the 19th Annual Meetings of Japan Society for Aeronautics and Space Sciences*, JASS, Tokyo, April 1988, pp. 87-88.

Compressed Polynomial Approach for Onboard Ephemeris Representation

B. V. Sheela* and P. Padmanabhan†
Indian Space Research Organization Satellite Centre, Bangalore, India

I. Introduction

ONBOARD ephemeris representation, be it for spacecraft pointing,[1] online annotation of remotely sensed imagery,[2] or NAVSTAR/global positioning system navigation message generation for a user satellite,[3] is becoming an increasingly important demand for any mission. In all of these cases, the end user is not only concerned with the accuracy of the ephemeris information but also the frequency and load of ground updates and onboard processing time. The alternatives for onboard ephemeris generation/representation known to date are 1) modeling of all the perturbative forces onboard,[4] 2) conic propagation using the delta-rho perturbation method,[5] 3) modeling of Keplerian parameters plus perturbations,[6] and 4) approximating the ephemeris by polynomials and transmitting the coefficients.[3]

As discussed in Ref. 4, although the first option allows more autonomy for the spacecraft, limited computing power onboard and ground update transmission limitations might render the approach unattractive sometimes. The second alternative, viz the delta-rho perturbation method,[5] is a very elegant approach, whose applicability to geosynchronous orbit has been demonstrated with simulation studies. In this method the trajectory of a desired orbit is treated onboard as a dispersion around a reference orbit, whose trajectory is generated in a large, ground-based computer and is transmitted to the spacecraft. Since this involves integration of differential equations, it may be beyond the capacity of the limited processing power of onboard processors. The third method, as stated in Ref. 6, does not abruptly deteriorate in accuracy after the duration of applicability but involves lengthy algorithms requiring large storage requirements. The suitability of the fourth option, namely polynomial approximation, has been demonstrated by Wakker et al.[3] for dissemination of NAVSAT ephemerides between both the mission center and the regional center as well as the regional center and user spacecraft. There the representation was restricted to parts of an orbit. All the same, the polynomial approach per se has been discarded by many[6] as being either incapable of representing multiple orbits or as too demanding in terms of transmission load when extended to multiple orbits. No evidence of exercising this computationally simple approach, with a view to compress the representation further, is seen in the literature, at least to the authors'

Received Oct. 26, 1988; revision received May 11, 1989.

*Scientist, Flight Dynamics Division.
†Division Head, Flight Dynamics Division.